



Ocean Surface Geostrophic Circulation Climatology and Annual Variations Inferred from Satellite Altimetry and GOCE Gravity Data

J. M. SÁNCHEZ-REALES,¹ M. I. VIGO,¹ and M. TROTTINI²

Abstract—We have studied, for the first time, variations in absolute surface geostrophic currents (SGC) using satellite data only. The proposed approach combines 18 years' altimetry data, which provide reliable measurements of absolute sea level (ASL), with a gravity field and steady-state ocean circulation explorer geoid model to obtain dynamic topography, and achieves unprecedented precision and accuracy. Our proposal overcomes the main limitations of existing approaches based solely on altimetry data (which suffer from lack of an independent reference for derivation of ASL maps), and approximations based on in-situ data (which are characterized by a sparse and inhomogeneous coverage in time and space). Features of annual variations of SGC are also addressed. As a result of our study we provide new absolute SGC climatology in the form of a 52-week data set of surface current fields, gridded at quarter degree longitude and latitude resolution and resolving spatial scales as short as 140 km. For presentation, this data set is averaged monthly and the results, presented as monthly climatology, are compared with climatology based on in-situ observations from drifter data.

Key words: Surface geostrophic circulation, dynamic topography, gravity field and steady-state ocean circulation explorer (GOCE), altimetry.

1. Introduction

Knowledge of variations of surface geostrophic currents (SGC) is crucial for understanding ocean dynamics, their driving mechanisms, and ocean mass and heat transport. In the recent past, ocean surface currents have mainly been estimated by use of drifter data from satellite-tracked drifters placed in all the ocean basins, within the global drifter program

(NILER *et al.* 2003; LUMPKIN and PAZOS 2007), which replaced historical ship drift (RICHARDSON 1989).

More recently, several studies have demonstrated the added value of altimetry data in study of the flow fields of the oceans. For example, SCHARFFENBERG and STAMMER (2010) showed the potential of the tandem mission Jason-TOPEX/Poseidon to enable understanding of the spatial structure of annual flow changes in a global context. Despite their unquestionable value, these contributions based on altimetry data are not suitable for study of absolute SGC, because they lack an independent estimate of the geoid for use as a reference for the altimetry-derived absolute sea level (ASL) maps.

The success of the gravity field and steady-state ocean circulation explorer (GOCE) mission has enabled this limitation to be overcome, because it provides an independent geoid representation with unprecedented spatial resolution. SÁNCHEZ-REALES *et al.* (2011, 2012), BINGHAM *et al.* (2011) and KNUDSEN *et al.* (2011) have recently proved the ability of GOCE to improve previous geodetic mean dynamic topography, and the corresponding benefits for ocean circulation studies.

In this paper we exploit these recent advances to estimate annual cycle and climatology of the major SGC in the oceans by combining 18 years altimetry data, which enable reliable measurement of ASL, with a GOCE geoid model to obtain a mean dynamic topography (DT) with unprecedented precision and accuracy. Our interest in annual variations is because these are the most relevant variations of SCG (at least for areas where the geostrophic flow is substantial).

The paper is organized as follows. Data and methodology are described in the next section. Annual climatology and cycle of SGC derived from altimetry and GOCE are discussed in the Sect. 7,

¹ Department of Applied Mathematics, University of Alicante, Alicante, Spain. E-mail: vigo@ua.es

² Department of Statistics and Operational Research, University of Alicante, Alicante, Spain.

where a comparison with the corresponding climatology and cycle obtained from in-situ measurements from drifter buoys is also presented. Concluding remarks are outlined in the Sect. 11.

2. Data and Methodology

2.1. Geoid

We use the third generation of GOCE data to determine the geoid; in particular, we use the earth gravity model (EGM) solution produced by the time-wise approach. The time-wise approach offers a GOCE-only model in a rigorous sense. That is, no external gravity field information is included, and thus the solution is solely based on GOCE data (PAIL *et al.* 2010, 2011). The GOCE gravity model is given after application of the usual corrections (EGG-C 2009; KURTENBACH *et al.* 2009). To match the grid of altimetry data we evaluate the GOCE geoid also in a quarter-degree grid.

Earth's gravity model solution is given as a set of normalized Stokes coefficients completed up to a maximum degree and order 232. This corresponds to a potential resolving power of approximately 86 km for the geoid. SÁNCHEZ-REALES *et al.* (2012) showed that, because of the nature of the GOCE, this resolution is sufficient to resolve the mean geostrophic flow for middle-to-high latitudes, but not for the equator, which remains a noisy band for which some filtering is needed (described in the Sect. 5).

2.2. Sea Surface Height

Weekly and monthly maps of absolute sea level are estimated by restoring the sea level anomalies (SLA) to the mean sea surface (MSS) of reference.

Sea level maps were provided by AVISO (<http://www.aviso.oceanobs.com>, downloaded 3 May 2011) as a weekly merged solution from several altimetry satellites (ERS-1/2, Topex/Poseidon (T/P), ENVISAT and Jason-1/2) for the time span 1992/10/14 to 2010/12/01. These maps are given as anomalies in relative to CLS01-MSS (HERNANDEZ

and SCHAEFFER 2001), which is provided with a two-degree resolution mesh. To obtain ASL from these anomalies, the CLS01-MSS was redistributed to a quarter-degree mesh via a 2D cubic splines interpolation, and added back to each SLA map to make feasible computation of the DT and their derived SGC. The usual corrections had already been applied to all data sets (SSALTO/DUACS USER HANDBOOK 2011).

For weekly climatology, data are redistributed (via weighted averages) to weeks corresponding to days 1–7, 8–14, ... and so on. Averaging the weekly maps, by week of the year, for the 18-year period from December 1992 to November 2010 yields the weekly climatology.

For monthly climatology, monthly maps were obtained as weighted averages of weekly maps from AVISO. This produces 18 maps for each month. The average of these monthly maps, by month, yields the monthly climatology.

2.3. Time-Variable Surface Geostrophic Currents

The absolute DT (ADT) map for each time (either weekly or monthly) is obtained by subtracting the geoid, N , from the corresponding absolute sea level map, i.e.:

$$\text{ADT}(t) = \text{ASL}(t) - N \quad (1)$$

where t represents time (in weeks or months). The ADT(t) in Eq. (1) can be readily expressed in the spectral domain (BINGHAM *et al.* 2008, HUGHES and BINGHAM 2006). Although SÁNCHEZ-REALES *et al.* (2012), proved that GOCE data can resolve space scales as short as 86 km for middle-to-high latitudes, solving for circulation at low latitudes requires a high level of filtering. Therefore, Gaussian smoothing of 140 km of half-wave length was applied to both the ASL(t) and N to ensure homogenization of the length scales and remove omission errors in the geoid (KNUDSEN *et al.* 2011).

The SGC speed $U_s = u_s + iv_s$ in terms of the zonal or eastward component, u_s , and the meridional or northward component, v_s , along the east (x), and north (y) directions, follows immediately via the geostrophic equation for the balance of the pressure gradient force and the Coriolis frequency:

$$\begin{aligned}
 u_s(t) &= -\frac{g}{f} \frac{\partial ADT(t)}{\partial y}, \\
 v_s(t) &= \frac{g}{f} \frac{\partial ADT(t)}{\partial x},
 \end{aligned}
 \tag{2}$$

where g is gravity, and $f = 2\Omega \sin \varphi$ is the Coriolis frequency, which depends on the latitude φ (Ω denotes the rate of rotation of the earth). The Coriolis frequency vanishes at the equator; therefore numerical computation of Eq. (2) becomes unstable when $\varphi \rightarrow 0$. We treat this problem by estimating the SGC for the equatorial band [5°S, 5°N] by following the methodology proposed in (LAGERLOEF *et al.* 1999). Let U_g denote the geostrophic component of the circulation:

$$\text{if } U_g = -gZ \tag{3}$$

where $U_g = u_g + iv_g$ and $Z = \frac{\delta ADT}{\delta y} + i \cdot \frac{\delta ADT}{\delta x}$. Denoting by U_β the geostrophic velocities computed with a β -plane approximation ($f = \beta \cdot y$), using the derivative of Eq. (3):

$$\beta U_\beta + \beta y \frac{\partial U_\beta}{\partial y} = ig \frac{\partial Z}{\partial y} \tag{4}$$

where $U_\beta = u_\beta + i v_\beta$ in the equatorial band. We approximate the solution of Eq. (4) by use of a polynomial expansion:

$$\begin{aligned}
 Z_\beta &= Z_0 + Z_1\varphi + Z_2\varphi^2 + Z_3\varphi^3 \\
 U_\beta &= \frac{ig}{\beta L} (Z_1 + Z_2\varphi + Z_3\varphi^2)
 \end{aligned}
 \tag{5}$$

where $L \approx 111$ km represents 1° at the equator. The SGC are then obtained by weighting U_s and U_β by:

$$(u_g, v_g) = \omega_\beta (u_\beta, v_\beta) + \omega_s (u_s, v_s) \tag{6}$$

where $\omega_\beta = 1$ and $\omega_s = 0$ at the equator, $\omega_\beta \rightarrow 0$ and $\omega_s \rightarrow 1$ at 5°N and 5°S . We defined the weighting functions as:

$$\begin{aligned}
 \omega_\beta &= \exp\left[-(\varphi/\varphi_c)^2\right] \\
 \omega_s &= 1 - \omega_\beta
 \end{aligned}
 \tag{7}$$

where the latitudinal length scale φ_c (here $\varphi_c = 2.2^\circ$) is selected to distribute the weights in Eq. (6).

2.4. Drifter Buoy Measurements

A monthly climatology for the ocean surface currents based on in-situ drifter buoy measurements is provided by the Global Drifter Program on a one degree grid covering latitudes between 73°S and 85°N (http://www.aoml.noaa.gov/phod/dac/drifter_climatology.html; LUMPKIN and GARRAFFO 2005; NIILER 2001; SYBRANDY and NIILER 1991). Drifter

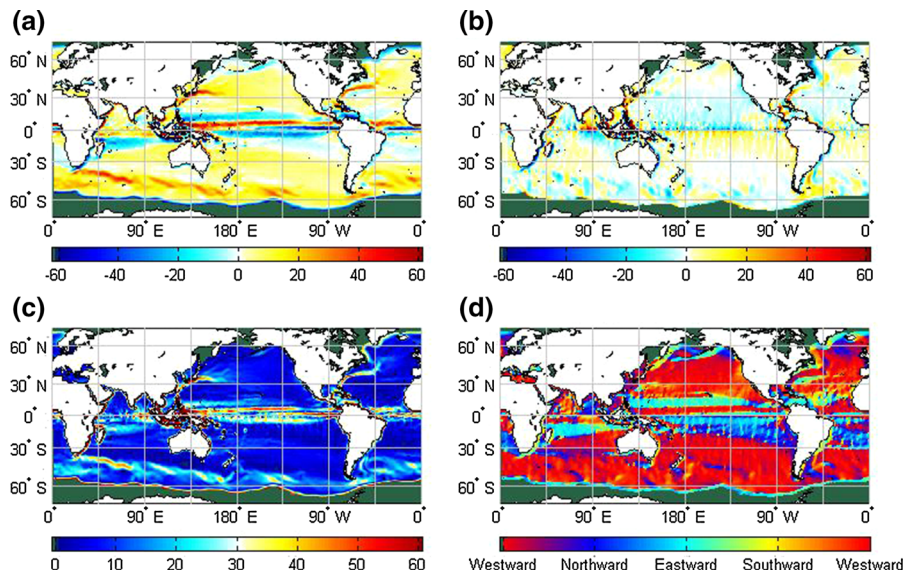


Figure 1

Annual mean SGC climatology estimated from altimetry and GOCE data: **a** zonal component; **b** meridional component; **c** velocity; **d** direction

observations include geostrophic currents and several other signals (tide currents, Ekman currents, inertial currents, and high-frequency ageostrophic currents), hence the drifter data must be corrected to achieve consistency for comparison with the geostrophic velocities derived from the geodetic DT. This solution is provided when daily winds from NCEP/NCAR re-analysis are interpolated on to the drifter positions and used to estimate and remove the slip associated with direct wind forcing (NILER and PADUAN 1995; PAZAN and NILER 2000). Wind stress and the local Coriolis frequency were used to estimate the Ekman component (RALPH and NILER 1999), which is subtracted to generate a separate Ekman-free surface geostrophic velocity field. Finally, a 5-day low pass filter was used to remove inertial and tidal currents and residual high-frequency ageostrophic currents.

Note that, in contrast with GOCE-derived currents, which are determined from a well-defined time span, the drifter observations are obtained from approximately a thousand drifters non-uniformly distributed in space and time. Therefore some artefactual discrepancies may be present when comparing the SGC estimates, particularly for areas with strong inter-annual to decadal variations (QIU and CHEN 2005).

3. Results

3.1. Climatology of Surface Geostrophic Currents

The annual mean climatology, which is an approximation to the mean SGC for the 18-year period, is shown in Fig. 1. Figure 1a, b show the

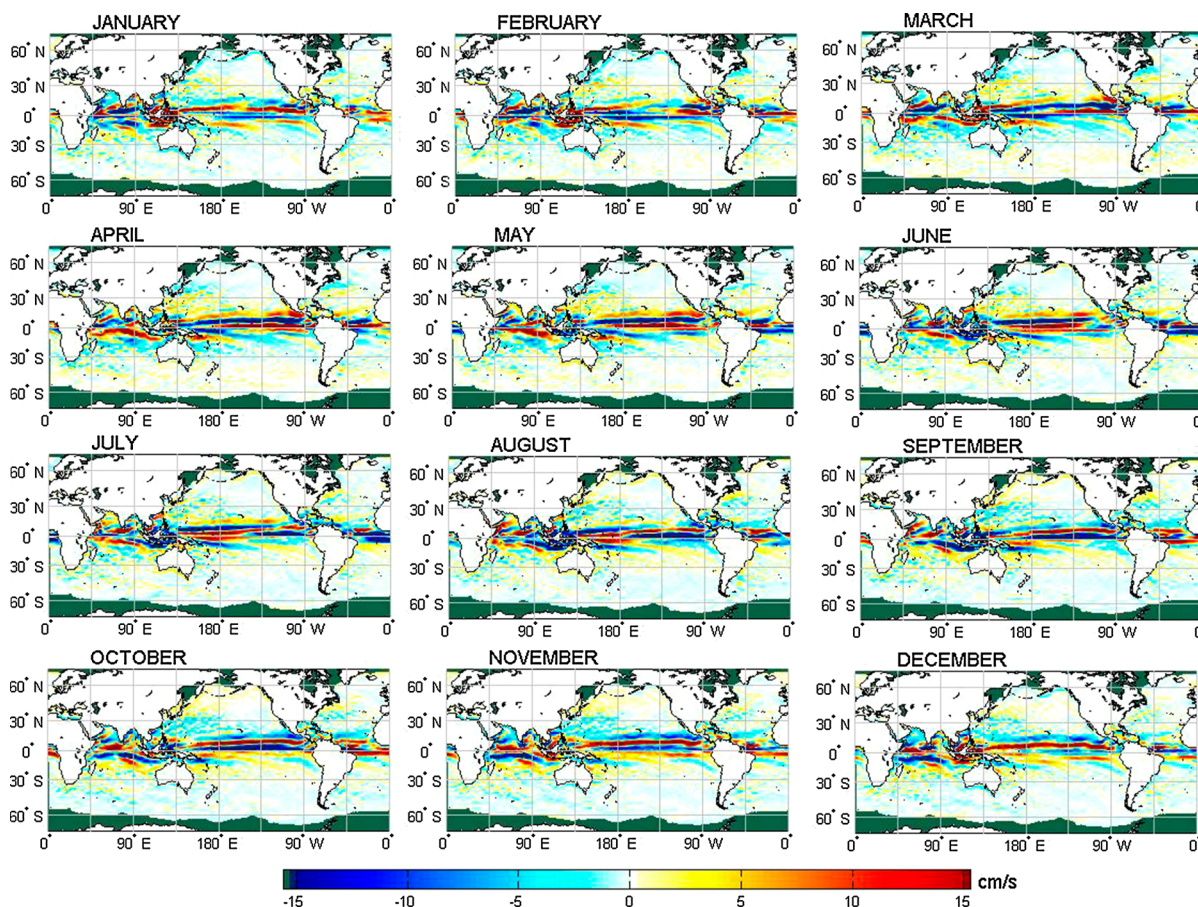


Figure 2

Monthly SGC climatology anomalies for the zonal component estimated from altimetry and GOCE data

zonal and meridional components of the SGC annual mean climatology in cm/s. The velocity map (cm/s) and the direction map for the annual mean climatology are presented in Fig. 1c, d. The results are in accordance with previous studies of the mean SGC (SÁNCHEZ-REALES *et al.* 2012; KNUDSEN *et al.* 2011). The estimated velocities, Fig. 1c, reach values higher than 40–50 cm/s in the western boundary currents, that is, the Kuroshio and the Gulf stream located at the North Pacific and North Atlantic Oceans, respectively. Large velocities higher than 30–40 cm/s are also observed at the Southern Ocean Circulation System, where the Antarctica Circumpolar Current and the Falkland current can be clearly identified. Equatorial currents are also well defined in the Pacific and Atlantic basins. To better illustrate monthly variations of the SGC the annual mean climatology,

shown in Fig. 1, is removed from the data. Figures 2 and 3 show monthly climatology anomalies for the zonal and the meridional components of the SGC, respectively. The strongest variations are observed in the zonal component along the low-latitude currents, for which velocities peak at more than 15 cm/s in absolute value. The three branches at the equatorial pacific formed by the north equatorial current, the equatorial counter current, and the south equatorial current are modulated in the seasonal cycle. These three currents can be identified clearly in October in the same direction as the mean flow. This is the month in which anomalies (with respect to annual mean climatology) are higher in the same direction than the mean flow, and, therefore, anomalies intensify the velocity of the mean current. From November, the anomaly flow remains in the direction

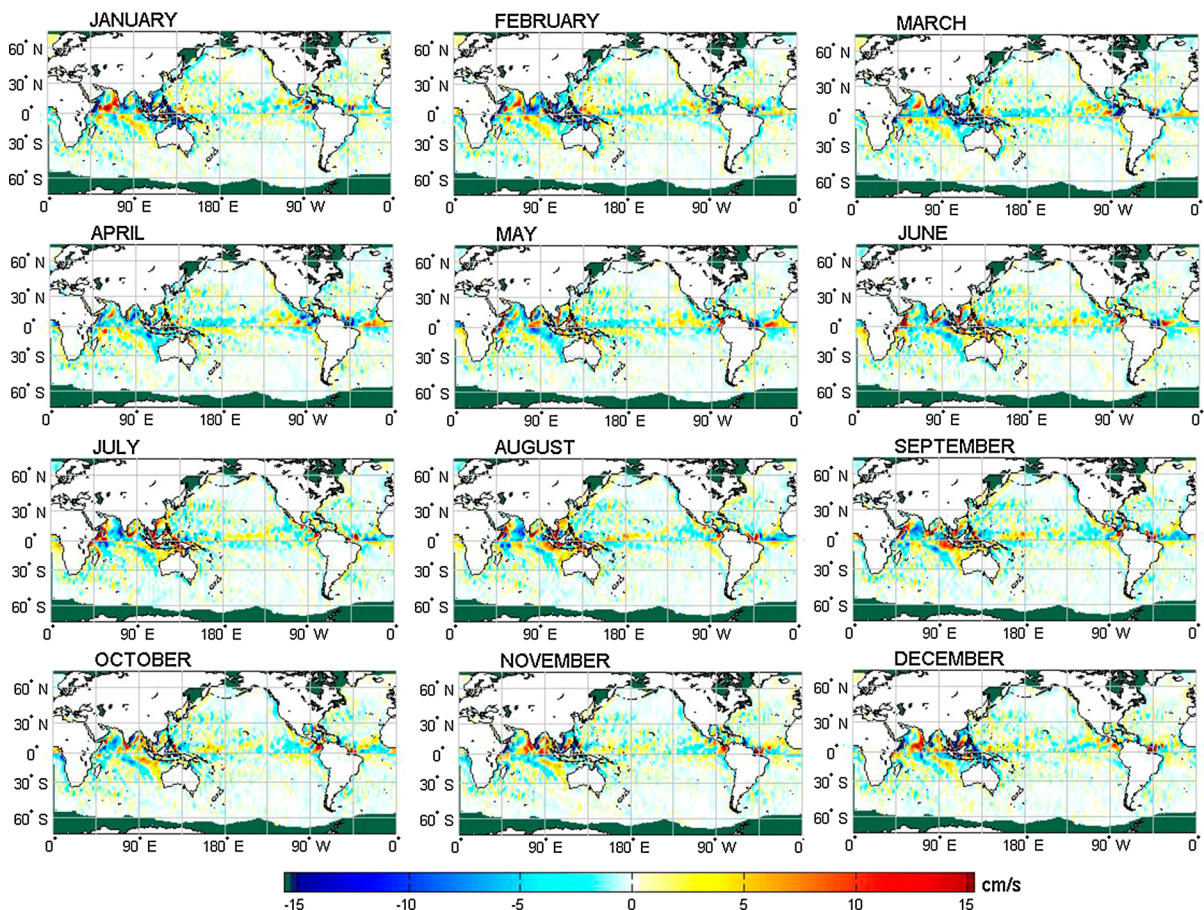


Figure 3

Monthly SGC climatology anomalies for the meridional component estimated from altimetry and GOCE data

of the mean flow but intensities decrease, becoming weaker and weaker throughout December–February until, in March, the anomalies flow is reversed and flows in the direction opposite to the mean flow for the three branches. This results in a decrease in the absolute velocity of these three currents (the mean flow is decelerated by the anomaly flow) through May to June, when anomalies reach the maximum velocity along the direction opposite to the mean flow. From June, velocities start to accelerate (with the anomalies turning into the mean flow direction) until they reach their maxima in September–October. For the meridional component, intensities are much smaller, except for the Kuroshio and Agulhas current. Most of activity accumulates in the main currents areas, the equator band, and the Indian Ocean. In the latter, seasonality is more prominent in the northern part than in the southern part.

Seasonal variability (standard deviation) of the geostrophic flow of the monthly SGC for both the zonal and the meridional components is shown in Fig. 4. Notice that the color scale is designed to

resolve regional features rather than extreme values and saturates at 15 cm/s. As expected from the strong annual cycle observed in Fig. 2, the equator band is the area with the highest variability for the zonal component (Fig. 4a) with peaks above 20 cm/s (saturated dark red in Fig. 4). However, significant variability can also be observed in the major current areas:

- the Kuroshio current running north-eastward being the boundary current in the North Pacific Ocean;
- the gulf stream flowing north-eastward along the North American coast being the boundary current in the North Atlantic Ocean; and
- the Antarctica Circumpolar Current along the Antarctica coast from south Africa to Australia

All reach values of approximately 10 cm/s. This high variability is related to the “chaotic” nature of these areas responding to shorter time-scale variations rather than to a clear seasonal cycle (Fu *et al.* 2010; Fu 2009, 2007). In opposition to the zonal map, the meridional component map

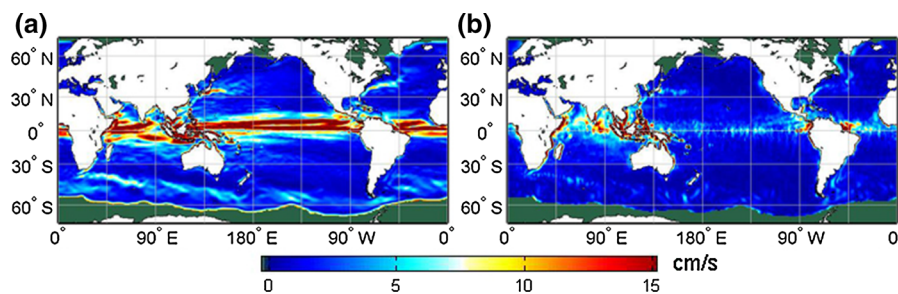


Figure 4

Standard deviation of the monthly SGC climatology estimated from altimetry and GOCE data: **a** zonal component; **b** meridional component

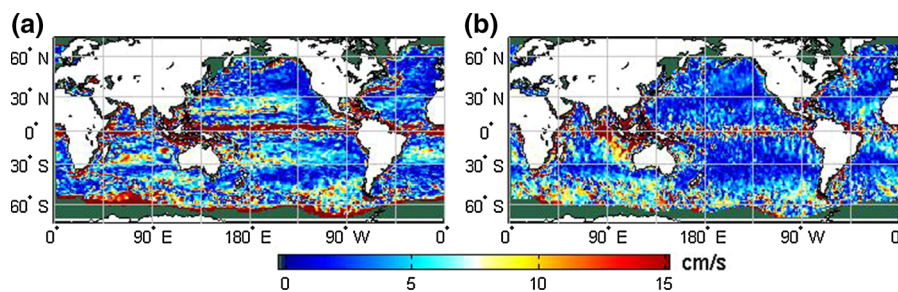


Figure 5

Absolute differences between annual mean SGC climatology estimated from altimetry and GOCE data and the corresponding climatology obtained from drifter data: **a** zonal component; **b** meridional component. The *color scale* is designed to resolve regional features rather than extreme values and saturates at 15 cm/s

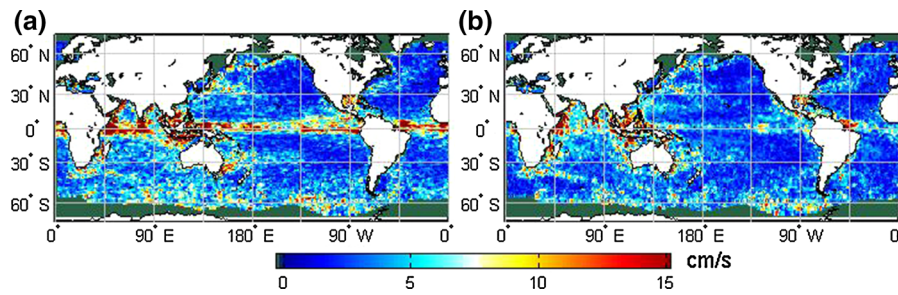


Figure 6

RMS differences between annual mean SGC from altimetry and GOCE data for the 18 years of this study, and the corresponding annual mean values obtained from drifter data: **a** zonal component; **b** meridional component

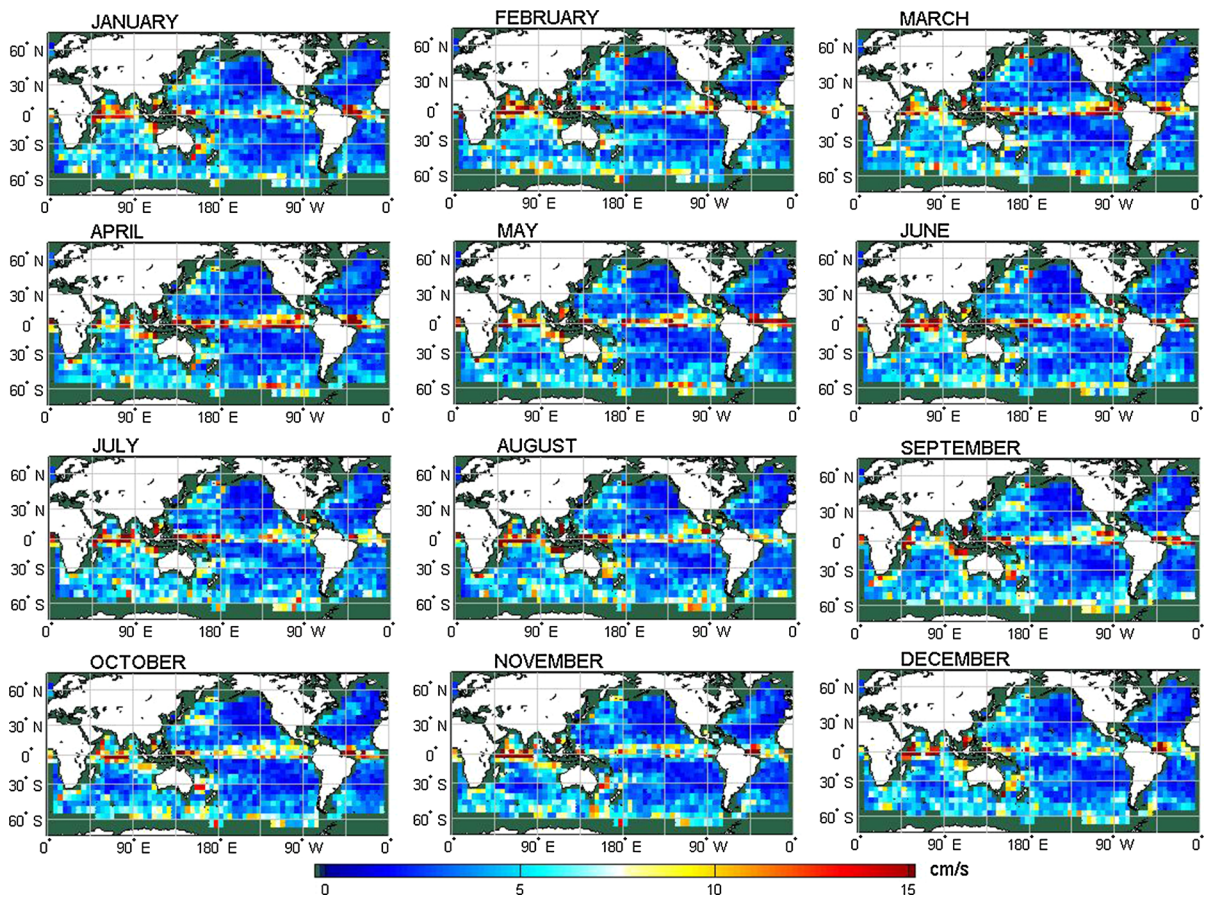


Figure 7

RMS monthly differences (for each 5° bin) between altimetry and GOCE and drifter-based SGC climatology for the zonal component

(Fig. 4b) shows much weaker variability reaching relatively high values in the Indian Ocean and the Equatorial Atlantic. The gulf stream and the Kuroshio currents can be discerned in the map but the Antarctic Circumpolar Current can barely be identified.

3.2. Comparison with Drifters

Climatology from altimetry and GOCE, shown in Figs. 1, 2 and 3, was compared with the resulting climatology obtained from drifter measurements. Figure 5 shows maps of absolute differences between

annual mean climatology from altimetry and GOCE (Fig. 1a, b) and the corresponding climatology obtained from drifters for both the zonal (Fig. 5a) and meridional (Fig. 5b) components of the flow. Notice that the color scale is designed to resolve regional features rather than extreme values and saturates at 15 cm/s. Differences larger than 15 cm/s (saturated to dark red in Fig. 5) are mainly observed in:

- a narrow equatorial band, partly because of the geodetic approximation to the geostrophic flow in this area (β -plane);
- the gulf stream; and
- the Southern circulation system where the observed differences could be because satellite altimeters have a weaker coverage of the sea

surface at higher latitudes, and drifter measurements are contaminated by strong winds and ocean waves (NILER *et al.* 2003).

Areas with absolute differences of 8–10 cm/s can be identified in the Southern Atlantic and North and South Pacific basins. These differences are located in areas where velocities are close to zero, and are mainly because of differences between zonal components estimated from satellite and drifter data. As shown by SÁNCHEZ-REALES *et al.* (2012), the estimated mean velocities obtained from both GOCE and GRACE data in combination with altimetry are higher than observed velocities from drifter data in these regions. This could be because small-scale circulation details are removed in the filtering process, but further studies are needed to confirm this.

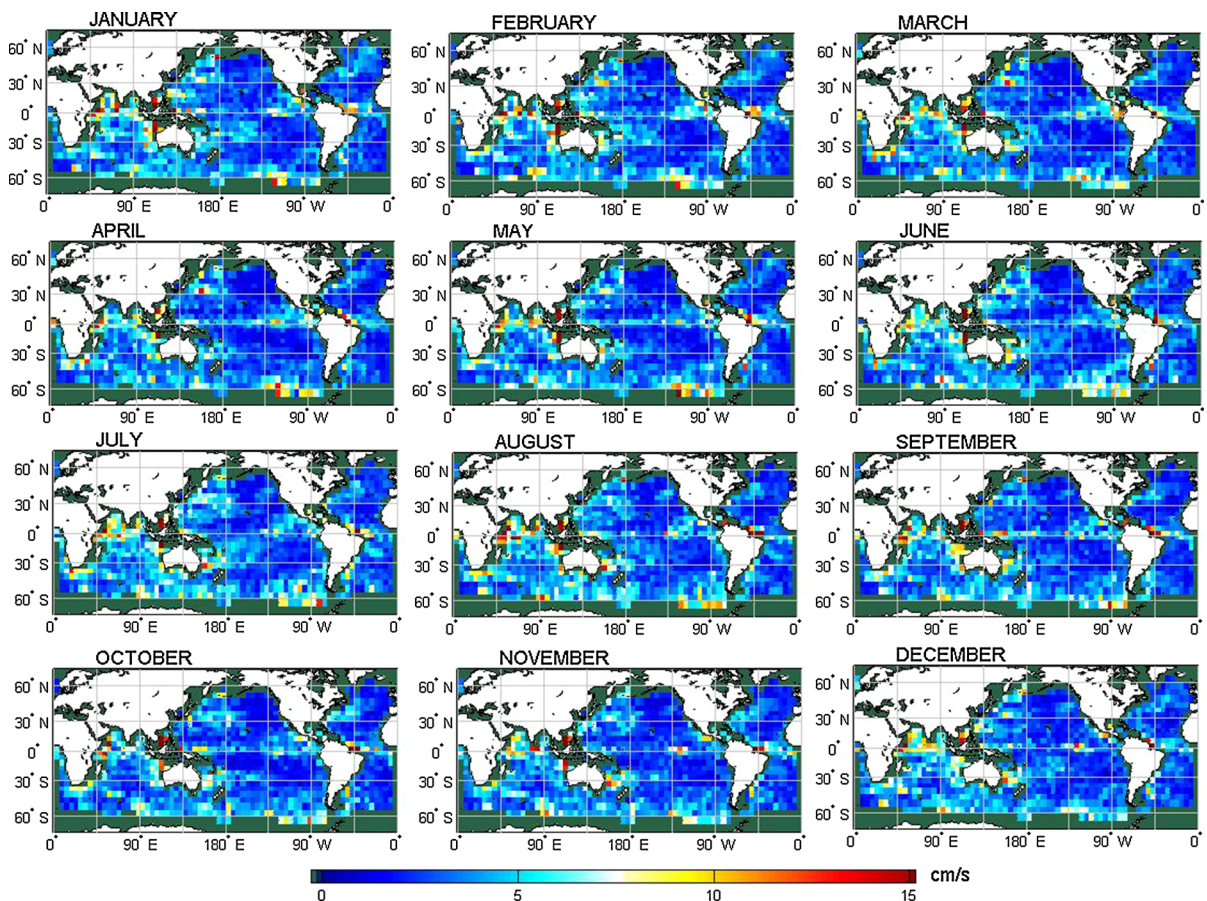


Figure 8

RMS monthly differences (for each 5° bin) between altimetry and GOCE and drifter-based SGC climatology for the meridional component

Figure 6a shows the root mean square (RMS) differences between annual mean values for the zonal component of the SGC from altimetry and GOCE data for the 18 years of this study and the corresponding annual mean values obtained from drifter data. The same information for the meridional component is shown in Fig. 6b. In general, RMS differences are smoother than absolute differences in Fig. 5, and remarkable differences (approx. 15 cm/s for the zonal component) are mainly located along the equatorial band and some coastal areas in the Indian Ocean. Climatology estimated from both datasets are in good agreement.

RMS (for each 5-degree bin) monthly differences between altimetry and GOCE and drifter-based climatology is shown in Figs. 7 and 8 for the zonal and meridional components, respectively. In general, higher RMS values coincide with larger anomalies (Figs. 2, 3) in both space and time, e.g. the equatorial Pacific Ocean in April–May, as could be expected.

The high RMS values observed in the North Indian Ocean can be explained by the geostrophic monsoon currents that do not form, or decay, across the basin all at once. Instead, patches of the currents appear or decay at different times. Higher RMS differences occur during the summer and winter monsoon currents whereas lower RMS values are observed for March–April and September, which are the transition months, in agreement with regional studies (SHANKAR *et al.* 2002). In contrast, the Antarctic Circumpolar Current is weakly identified, by RMS differences of approximately 5 cm/s (differences here could be because of the same factors as for the mean SGC).

3.3. Annual Variations

The amplitudes of the annual cycle, estimated as half the range of the climatology, in the zonal (u) and meridional (v) components of the flow are shown in Fig. 9a, d respectively. As expected, spatial

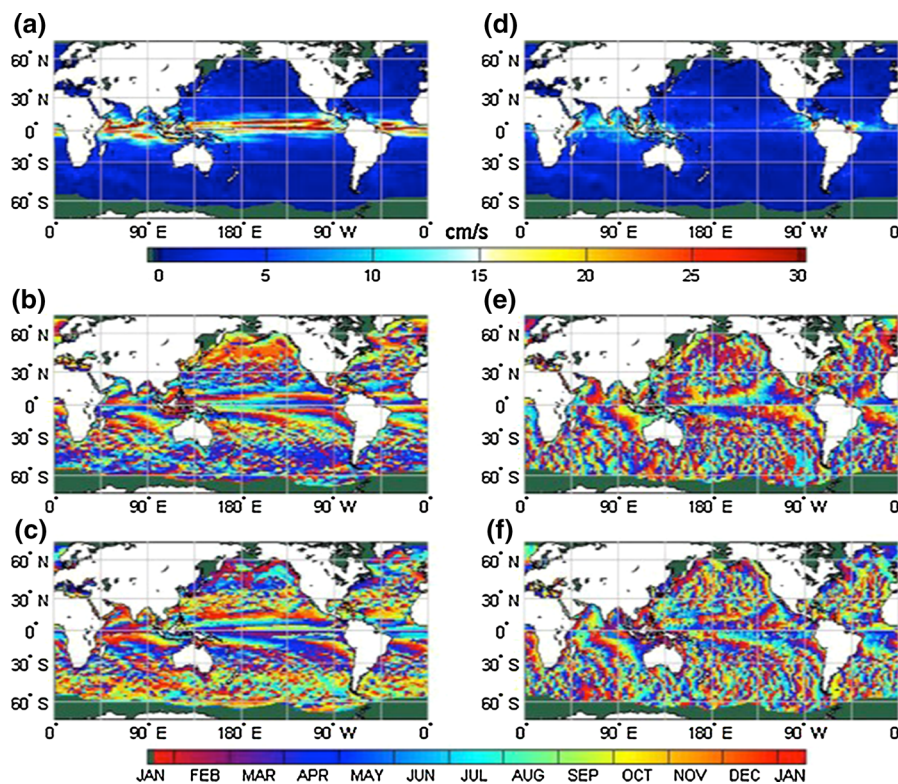


Figure 9

Annual variation of SGC derived from altimetry and GOCE. Annual amplitude, half range: **a** zonal component; **d** meridional component. Month at which the maximum is achieved: **b** zonal component; **e** meridional component. Month at which the minimum is achieved: **c** zonal component; **f** meridional component

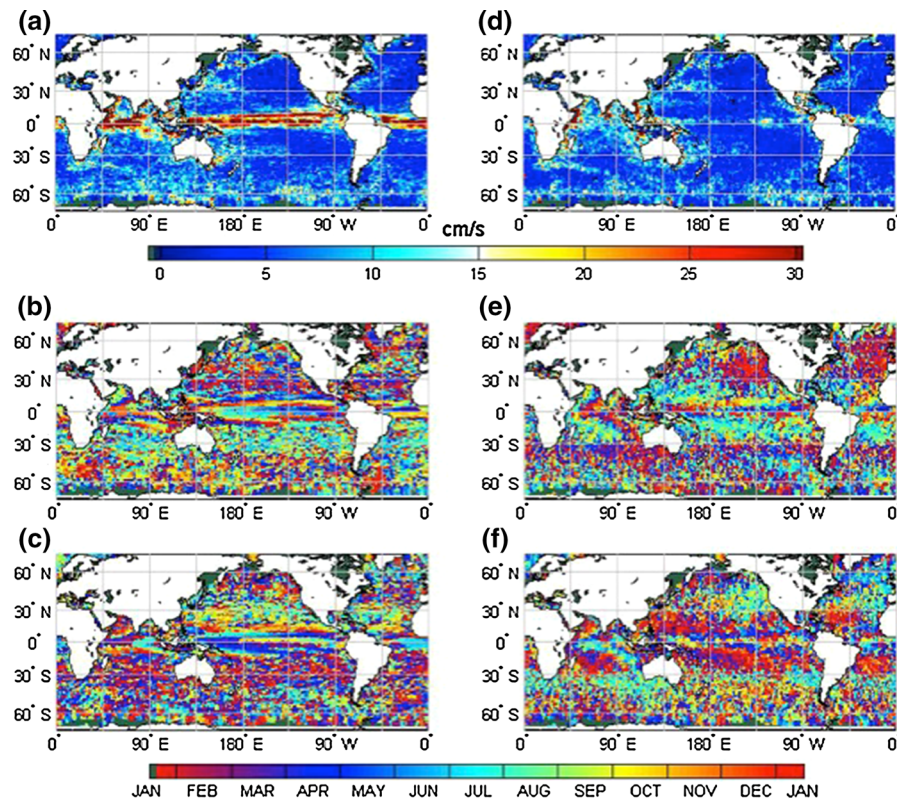


Figure 10

Annual variation of SGC as measured by use of drifters. Annual amplitude, half range: **a** zonal component; **d** meridional component. Month at which the maximum is achieved: **b** zonal component; **e** meridional component. Month at which the minimum is achieved: **c** zonal component; **f** meridional component

distribution of the annual amplitude reflects the corresponding distribution of the standard deviation in Figs. 4a, b. Except for the equator band, the major current areas are characterized by very low seasonal amplitudes, because intra-seasonal variability in these areas is a result of higher time-frequencies rather than a strong annual harmonic.

For the zonal component, most of major equatorial currents—the equatorial counter current (ECC), the north equatorial current (NEC), and the south equatorial current (SEC)—seasonal amplitudes are higher than 20 cm/s, with values up to 40 cm/s at some regions mainly for the ECC. Notice that the color scale is designed to resolve regional features rather than extreme values and saturates at 30 cm/s. In contrast, the meridional component seems to be characterized by a much weaker annual cycle, with the highest amplitudes (>10 cm/s) in the Western Equatorial Atlantic, the ECC in the Indian Ocean, and Agulhas currents.

Figures 9b, e show the months in which the maximum value in the seasonal cycle is reached at each location for the zonal and the meridional components of the geostrophic flow. Similarly, Figs. 9c, f show the months in which the minimum value in the seasonal cycle is reached at each location for the zonal and meridional components of the geostrophic flow. These maps might be interpreted as the phase of the seasonal cycle. Areas of interest are those in which the seasonal cycle is significant. It is apparent that areas characterized by the strongest amplitudes in the Indian ocean reach their maximum values in opposite phases—approximately December in the northern hemisphere and approximately May in the southern hemisphere. The sense of the circulation is clearly captured for the Eastern Equatorial Pacific where some kind of propagation can be appreciated at the NEC-ECC system.

Seasonal cycle results based on altimetry and GOCE are in good agreement with similar results

based on drifter data, shown in Fig. 10. Amplitudes and pattern distribution (Fig. 10a, d) agree well for low latitudes. Nevertheless, drifter data furnish larger seasonal cycles for the Kuroshio, Gulf Stream, and Antarctic Circumpolar Current than the altimetry and GOCE. This is because solving the SGC on the global scale requires a high level of filtering to solve the equator band. In this instance we used a Gaussian filter of 140 km half-wave length, which removes small-scale circulation details in these areas.

4. Conclusions

In this work, for the first time, we have obtained weekly and monthly SGC climatology using only satellite data from altimetry and GOCE missions. The proposed approach combines 18 years of altimetry data with an independent estimate of the geoid based on the third release of GOCE data. Our approach overcomes the main limitations of existing approaches based solely on altimetry data (which suffer from lack of an independent estimate of the geoid which can be used as a reference for the altimetry-derived ASL maps), and approximations based solely on in-situ data (which are characterized by sparse and inhomogeneous coverage in time and space).

The annual variations of the SGC that we report are in agreement with several regional studies, and enable them to be placed in a global context. High, significant variability is observed for the SGC for the equator band and for the major current areas (the Kuroshio, Gulf Stream, ACC, and the Malvinas currents) mainly because of the zonal component. Most of this variability is related to inter-seasonal variations except for some areas in the equator band, as is also observed for the Eastern Pacific and the Atlantic Ocean, where the seasonal cycle explains most of the variance of the currents.

Our study shows the annual cycle is very strong for the equatorial band of the zonal component. The NEC, ECC, and NECC are clearly identified by seasonal amplitudes $>20\text{--}30$ cm/s. The estimated climatology is in general agreement with that obtained from in-situ drifter buoy measurements.

Study of variability on a smaller scale would require finer resolution of the geoid and use of more

advanced filtering methods. Further research on anisotropic filters could provide a useful tool to address these problems.

REFERENCES

- BINGHAM R., HAINES K., and HUGHES C. (2008) *Calculating the ocean's mean dynamic topography from a mean sea surface and a geoid*, J Atmos Ocean Tech, 25(10),1808–1822. doi:10.1175/2008JTECHO568.1.
- BINGHAM RJ., KNUDSEN P., ANDERSEN O., and PAIL R. (2011) *An initial estimate of the North Atlantic steady-state geostrophic circulation from GOCE*. Geophys Res Lett, 38:L01606. doi:10.1029/2010GL045633.
- EGG-C (EUROPEAN GOCE GRAVITY CONSORTIUM) (2009). GOCE high level processing facility: GOCE level 2 product data handbook. GO-MA-HPF-GS-0110.
- FU, L.-L., CHELTON, D.B. LE TRAON P.-Y., and MORROW R. (2010). *Eddy dynamics from satellite altimetry*. Oceanography 23(4):14–25.
- FU, L.-L. (2009), *Pattern and velocity of propagation of the global ocean eddy variability*, J. Geophys. Res., 114, C11017, doi:10.1029/2009JC005349.
- FU, L.-L. (2007), *Intraseasonal Variability of the Equatorial Indian Ocean Observed from Sea Surface Height, Wind, and Temperature Data*. J. Phys. Oceanogr., 37, 188–202.
- HERNANDEZ F. and SCHAEFFER P. (2001). The CLS01 MSS: A validation with the GSFC00.1 surface. Tech. rep., CLS, Ramonville St Agne, 14 pp.
- HUGHES, C. and BINGHAM, R. (2006). *An oceanographers guide to GOCE and the geoid*. Ocean Sci. Discuss., 3, 1543–1568. doi:10.5194/osd-3-1543-2006.
- KNUDSEN, P., ANDERSEN O., BINGHAM R. and RIO M.-H. (2011), *A global mean dynamic topography and ocean circulation estimation using a preliminary GOCE gravity model*. J. Geodesy, doi:10.1007/s00190-011-0485-8.
- KURTENBACH, E., MAYER-GÜRR T., and EICKER, A. (2009). *Deriving daily snapshots of the Earth's gravity field from GRACE LIB data using Kalman filtering*, Geophys. Res. Lett., 36, L17102, doi:10.1029/2009GL039564.
- LAGERLOEF, G. S. E., G. T. MITCHUM, R. B. LUKAS, and P. P. NIILER (1999), *Tropical Pacific near-surface currents estimated from altimeter, wind, and drifter data*, J. Geophys. Res., 104(C10), 23, 313–23, 326, doi:10.1029/1999JC900197.
- LUMPKIN R., and GARRAFFO Z., (2005) *Evaluating the Decomposition of Tropical Atlantic Drifter Observations*. J Atmos Ocean Techn I 22, 1403–1415. doi:10.1175/JTECH1793.1.
- LUMPKIN, R., and M. PAZOS, (2007), *Measuring surface currents with Surface Velocity Program drifters: the instrument, its data, and some recent results*, Chapter 2 of “Lagrangian Analysis and Prediction of Coastal and Ocean Dynamics”, ed. A. Griffa, A. D. Kirwan, A. Mariano, T. Özgökmen, and T. Rossby, Cambridge University Press.
- NIILER, P. P. and J. D. PADUAN (1995), *Wind-driven motions in the northeast Pacific as measured by Lagrangian drifters*. J. Phys. Oceanogr. 25, 2819–2830.
- NIILER, P. P., (2001), *The world ocean surface circulation*. In Ocean Circulation and Climate, G. Siedler, J. Church and J. Gould, eds., Academic Press, Volume 77 of International Geophysics Series, 193–204.

- NIILER, P. P., N. A. MAXIMENKO and J. C. McWILLIAMS, (2003), *Dynamically balanced absolute sea level of the global ocean derived from near-surface velocities observations*. Geophys. Res. Lett., 30(22) 2164, doi:10.1029/2003GRL018628.
- PAIL R., GOINGER H., MAYRHOFFER R., SCHUH W.D., BROCKMANN J.M., KRASBUTTER I., HÖCK E., and FECHER T. (2010) GOCE gravity field model derived from orbit and gradiometry data applying the time-wise method. Proc. ESA Living Planet Symposium. Bergen, Norway, 28 June-2 July 2010 (ESA SP-686, December 2010).
- PAIL R., BRUINSMAS S., MIGLIACCIO F., FOERSTE C., GOINGER H., SCHUHAND W.D., HOECK E., REGUZZONI M., BROCKMANN J.M., ABRIKOSOV O., VEICHERTS M., FECHER T., MAYRHOFFER R., KRASBUTTER I., SANSO F., and TSCHERNING C. (2011) *First GOCE gravity field models derived by three different approaches*. J Geodesy, 85:819–843. doi:10.1007/s00190-011-0467-x.
- PAZAN, S. E. and P. P. NIILER, (2000), *Recovery of near-surface velocity from undrogued drifters*. J. Atmos. Oceanic Technol. 18, 476–489.
- QIU B. and S. CHEN, (2005), *Variability of the Kuroshio extension jet, recirculation gyre, and mesoscale eddies on decadal time scales*. J. Phys. Oceanogr., 35, 2090–2103.
- RALPH, E. A. and P. P. NIILER, (1999), *Wind-driven currents in the Tropical Pacific*. J. Phys. Oceanogr. 29, 2121–2129.
- RICHARDSON, P. L. 1989. *Worldwide ship drift distributions identify missing data*. J. Geophys. Res. 94(C5):6169–6176, doi:10.1029/JC094iC05p06169.
- SÁNCHEZ-REALES, J. M., VIGO, M. I., JIN, S. G., and CHAO, B. F. (2011), *Global Surface Geostrophic Currents from Satellite Altimetry and GOCE*. Proc. 4th International GOCE User Workshop. Munich, Germany, 31 March–1 April 2011 (ESA SP-696, July 2011).
- SÁNCHEZ-REALES, J.M., VIGO, M.I., JIN, S.G., and CHAO, B.F. (2012), *Global Surface Geostrophic Ocean Currents Derived from Satellite Altimetry and GOCE Geoid*. Marine Geodesy. 35:sup1, 175–189.
- SCHARFFENBERG, M. G., and D. STAMMER, (2010), *Seasonal variations of the large-scale geostrophic flow field and eddy kinetic energy inferred from the TOPEX/Poseidon and Jason-1 tandem mission data*, J. Geophys. Res., 115, C02008, doi:10.1029/2008JC005242.1.
- SHANKAR D., P.N. VINAYACHANDRAN, and A.S. UNNIKRISHNAN, (2002), *The monsoon currents in the north Indian Ocean*. Progress in Oceanography 52, 63–120.
- SSALTO/DUACS USER HANDBOOK (2011) M(SLA) and M(ADT) Near-Real Time and Delayed-Time. SALP-MU-P-EA-21065-CLS.
- SYBRANDY, A. L. and P. P. NIILER, (1991), *WOCE/TOGA Lagrangian drifter construction manual*. WOCE Rep. 63, SOI Ref. 91/6, 58 pp, Scripps Inst. of Oceanogr., La Jolla, Calif.

(Received March 28, 2014, revised October 10, 2014, accepted November 4, 2014, Published online November 29, 2014)